Journal of Zhejiang University-SCIENCE A (Applied Physics & Engineering)
ISSN 1673-565X (Print); ISSN 1862-1775 (Online)
www.zju.edu.cn/jzus; www.springerlink.com
E-mail: jzus@zju.edu.cn

Optimization of cross angle based on the pumping dynamics model*

Ji-en MA[1], You-tong FANG[†‡1], Bing XU[2], Hua-yong YANG[2]

([1]*School of Electrical Engineering, Zhejiang University, Hangzhou 310027, China*)

([2]*State Key Lab of Fluid Power Transmission and Control, Zhejiang University, Hangzhou 310027, China*)

[†]E-mail: youtong@zju.edu.cn

Received July 8, 2009; Revision accepted Oct. 23, 2009; Crosschecked Jan. 22, 2010

Abstract: The single cylinder and multi-cylinder pumping dynamics model of a swash plate piston pump were improved. Particular attention has been paid to the design influences of key parts of the valve plate such as relief groove, pre-compression/expansion and fluid inertia effect of the unsteady flow. Some important parameters, such as the discharge area, discharge coefficient, fluid bulk modulus, were especially analyzed using numerical methods or by experiment-based estimation. Consequently, the mathematical results of pressure pulsation and flow ripple agree well with experimental results from the test-rig of the flow ripple. Therefore, the cross angle and the pre-compression angle of the valve plate was optimized, based on the pumping dynamics model. Considering both the flow ripple and the cylinder pressure of the pump, the cross angle is set to be 2.2° to 2.7° with a pre-compression angle of 1.7° to 2.2°, so the pumping dynamics character can obtain the best result.

Key words: Flow ripple, Pressure pulsation, Piston pump, Noise
doi:10.1631/jzus.A0900417 **Document code:** A **CLC number:** TP211.3

1 Introduction

An axial piston pump, the most important component in hydraulic systems, is widely used in the fluid power industry for its robustness, controllability, wide operating range and compact size. Noise level, one of the three important performance criteria of a piston pump, except for the service life and efficiency, is mainly produced by pumping dynamics, especially the flow ripple and cylinder pressure overshoots or undershoots. Pumping dynamics, such as flow ripple and cylinder pressure of the pump, is mainly created when fluid is forced from the low-pressure side to the high-pressure side, which is seriously affected by the valve plate design (Ericson and Palmberg, 2007). Besides, pumping dynamics can produce much damage to the pump, such as noise, lower volumetric efficiency, the tipping and overturning moment ripple on the cylinder block, cavitations, and short service life (Manring and Zhang, 2001; Manring and Dong, 2003). Therefore, it is necessary to study the pumping dynamics characteristics, and the valve plate design should be optimized to reduce the noise level of the pump.

To improve performance and increase the ratings of an axial piston pump, many different aspects of pump design have received attention. For example, pressure distribution, temperature, friction of the oil film between piston and cylinder block have been investigated by Lasaar and Ivantysynova (2001), Ivantysynova and Huang (2002) and Huang and Ivantysynova (2003). Advances in materials technology have improved contamination tolerance and fatigue technology (Bebber and Murrenhoff,

‡ Corresponding author

* Project supported by the National Key Technologies Supporting Program of China during the 11th Five-Year Plan Period (Nos. 2006BAF01B01, 2006BAF01B04, and 2007AA03Z211), the National Natural Science Foundation of China (No. 50877070), and the Technological Research and Development Programs of the Ministry of Chinese Railways (No. 2009J006-L)

2002; Bobzin *et al*., 2004). A significant amount of work has been carried out on piston slip behavior (Kazama, 2005; Rokala *et al*., 2008). In addition, flow ripple testing has been studied by Edge and Johnston (1990a; 1990b) and more recently by Liselott (2005). Therefore, pumping dynamics is a hot topic today and research institutes have carried out much research work in this area. Software DSHplus was used to simulate the flow ripple and cylinder pressure during the trapping period between valve plate ports of a piston pump by TU Aachen (Sanchen, 2003). TU Dresden (Becher, 2004) developed a computer model of the pressure and flow in an axial piston pump, and the ring flexibility structure of the pump was analyzed to reduce flow ripple. A single cylinder model was developed by Bath University using the oil momentum model in the silencing groove of the valve plate (Edge and Darling, 1988). This work was supported by an experimental study, and the accuracy on overshoot in cylinder pressure was improved. Ivantysynova and Huang (2005) developed a computer model of piston pump using an oil compressibility model. Moreover, the pumping dynamics character was studied using computational fluid dynamics (CFD) simulation (Meincke and Rahmfeld, 2008; Wustmann *et al*., 2008). The pumping dynamics of an axial piston pump was studied recently using DSHplus and MATLAB software (Guo and Wang, 1996; Lu, 2006). Also, valve plate design and lubrication have been studied by Na and Yin (2002) using a single cylinder model and the structure of relief grooves was analyzed.

This paper is concerned with the pumping dynamics of a swash plate piston pump, with emphasis on the cross angle design of the valve plate. The pumping dynamics model of the pressure and flow in a multi-cylinder pump was improved. And the cross angle design of the valve plate was optimized to reduce the noise level of the pump.

2 Modeling of pumping dynamics

2.1 Single cylinder model of pumping dynamics

In the study of the pumping dynamics of an axial piston pump, the single cylinder model of pumping dynamics was improved.

Fig. 1 shows a piston as it operates within its bore where the volume of fluid within the bore is taken as the control volume of the study. The pressure-rise-rate equation for the control volume within a piston chamber (Fig. 1) may be derived based upon the conservation of mass and the definition of the fluid bulk modulus. This result is given by Ivantysyn and Ivantysynova (2001):

$$\frac{\mathrm{d}p_\mathrm{f}}{\mathrm{d}t}=\frac{K_\mathrm{e}}{V_\mathrm{f}}(q_\mathrm{r}+q_\mathrm{i}-q_\mathrm{g}-q_\mathrm{l}), \tag{1}$$

where p_f is the pressure in piston chamber, t is the time, K_e is the fluid bulk-modulus, V_f is the instantaneous volume of the piston chamber itself, q_r is the volumetric flow rate bring by the motion of piston in the cylinder, q_i is the reverse flow because of pressure differential between the cylinder and kidney port, q_g express the fluid inertia effect in the unsteady flow, and q_l is the volumetric loss.

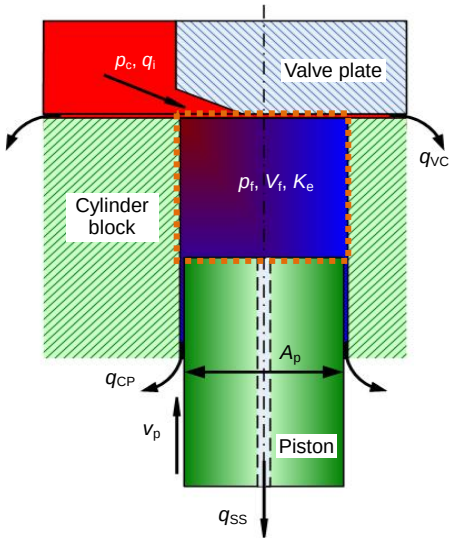

Fig. 1 A piston within a piston chamber

p_c: pressure in kidney port; q_{CP}: leakage flow between piston and cylinder block; q_{SS}: leakage flow between swash plate and slipper; q_{VC}: leakage flow between cylinder block and valve plate; q_{CP}: leakage flow between piston and cylinder block; v_p: velocity of piston; A_p: cross section of piston

The flow rate q_i is modeled using the classical orifice equation, which is written as

$$q_\mathrm{i}=C_\mathrm{i}A_\mathrm{i}\sqrt{2|p_\mathrm{c}-p_\mathrm{f}|/\rho}\cdot\mathrm{sign}(p_\mathrm{c}-p_\mathrm{f}), \tag{2}$$

where ρ is the oil density, p_c is the pressure in kidney port, which repeatedly changes from the discharge pressure to the intake pressure with the cylinder block rotating around the axis of the pump.

The discharge coefficient, C_i, is an uncertain parameter and varies with the flow condition. So the CFD software FLUENT is used to confirm this parameter by analyzing the flow condition inside the axial piston pump. The simulated pump with the mesh is shown in Fig. 2. The simulation model is improved by adding the compressible model of the fluid oil using the user defined function, which greatly improves the accuracy of the simulation. The flow in and out of the piston bore at the relief groove occurs at a high velocity with a high Reynolds number, with a velocity of around 100 m/s. The fluid situation is turbulent at this point. So the discharge coefficient at the relief groove is calculated based on the flow rate and pressure drop through the relief groove and it is about 0.75 according to simulation calculation (Fig. 3).

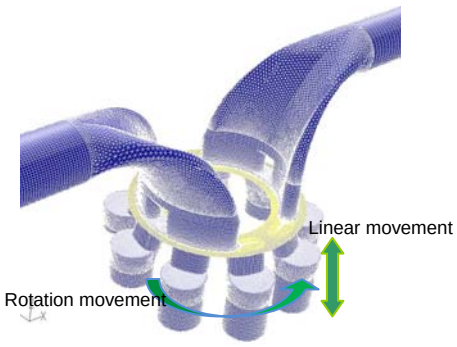

Fig. 2 Simulated pump with mesh

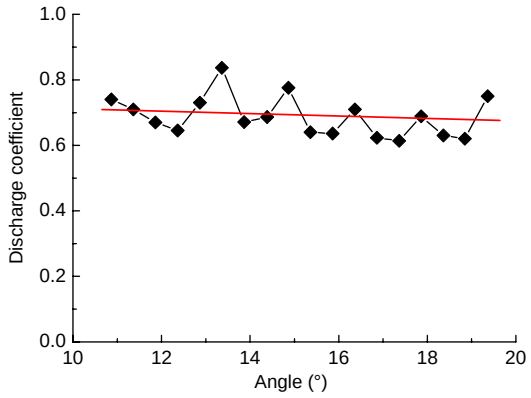

Fig. 3 Discharge coefficient simulation result

The discharge area of the piston bore, A_i, also varies with time to model the transition regions on the valve plate where the slots provide a variable opening into each port. The geometrical cross-sectional area is dependent on the position of the kidney-shaped flow passage from a single piston chamber and the discharge port on the valve plate, as shown in Fig. 4.

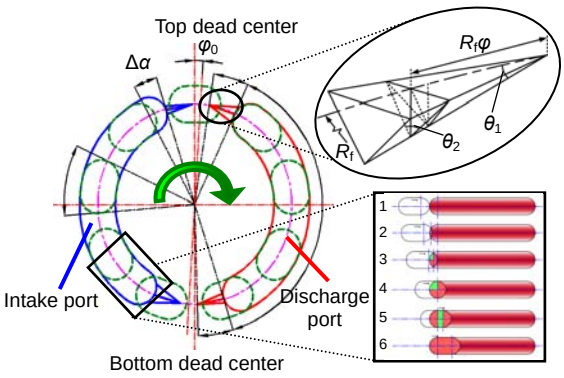

Fig. 4 Relationship between piston chamber and valve plate kidney bore

When the flow passage from a single piston chamber overlaps with the triangular relief groove, the geometry of the opening discharge area is a triangle which can be evaluated with

$$A_i = R_f r\varphi \sin\theta_1 \arctan\left(R_f\varphi \cdot \mathrm{tg}\theta_1 \mathrm{tg}\left(\frac{\theta_2}{2}\right)/r\right), \quad (3)$$

where R_f is the distribution radius of relief groove, r is the width radius of kidney port, φ is the position angle of piston, θ_1 and θ_2 are the depth and width angles of triangular relief groove, respectively.

When the overlapping position of the piston chamber and valve plate kidney bore appear from zone 1 to zone 4, the instantaneous discharge area generated by the superimposition of the valve plate port and the cylinder block port is olivary and is calculated by

$$A_i = (\varphi R - 2r)\sqrt{\varphi R r - \frac{\varphi^2 R^2}{4}} + 2r^2 \arcsin\left(\frac{\varphi R - 2r}{2r}\right) + \pi r^2, \quad (4)$$

where R is the kidney port/piston distribution radius.

With an instantaneous throat area from zone 4 to zone 6, the variational cross-sectional area is a rectangle:

$$A_i = \pi r^2 + 2r(\varphi - 2\Delta\alpha)R, \quad (5)$$

where $\Delta\alpha$ is the transition angle of kidney port.

Then the whole cylinder block port overlaps to the valve plate port and the cross section remains

constant. So the discharge area around the whole cycle was built based on the above analysis. Sixteen subsection functions should be used to evaluate the flow area of the valve plate in Fig. 4.

To account for fluid momentum effects, the effective mass of fluid to be accelerated is assumed to be contained within the relief groove. The fluid inertia effect in the unsteady flow is a nonlinear differential equation, written as

$$\frac{\mathrm{d}q_\mathrm{g}}{\mathrm{d}t}=\left(\frac{p_\mathrm{c}-p_\mathrm{f}}{\rho}-\frac{q_\mathrm{g}^2}{2C_\mathrm{i}^2A_\mathrm{i}^2}\right)\Bigg/\int_{x_1}^{x_2}\frac{1}{A_\mathrm{i}(x)}\mathrm{d}x, \tag{6}$$

where x_1, x_2 are the overlap linear positions of valve plate, respectively, as shown in Fig. 5.

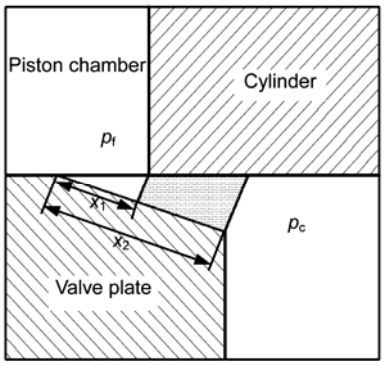

Fig. 5 Fluid inertia effect area in relief groove

The flow rate bring about by the motion of the piston is determined using the kinematics of the piston. This quantity is expressed as

$$q_\mathrm{r}=A_\mathrm{p}R\omega\sin\varphi\tan\beta, \tag{7}$$

where q_r is the flow change bring by the motion of piston, A_p is the cross section of piston, ω is the rotation speed of pump, and β is the swash plate angle.

The flow rate of volumetric loss, q_l, is the sum of the leakage flow through the gap between the piston and cylinder block, q_CP, and through the swash plate and the slipper, q_SS. The leakage flow through the gap between the cylinder block and valve plate, q_VC, is the effect of the multi-piston, and can only be considered in a multi-cylinder pump model. The model of leakage flow is give by (Ivantysyn and Ivantysynova, 2001)

$$q_\mathrm{CP}=\frac{\pi d_\mathrm{p}\delta_1^3}{12\mu l_1}(p_\mathrm{f}-p_0)-\frac{\pi d_\mathrm{p}\delta_1 v_\mathrm{p}}{2}, \tag{8}$$

$$q_\mathrm{SS}=\frac{\pi d_\mathrm{d}^4\delta_2^3}{\mu[6d_\mathrm{d}^4\ln(r_2/r_1)+128\delta_2^3 l_\mathrm{d}]}(p_\mathrm{f}-p_0), \tag{9}$$

$$q_\mathrm{VC}=\frac{\delta_3^3}{12\mu}\left[\frac{1}{\ln(R_2/R_1)}+\frac{1}{\ln(R_4/R_3)}\right](p_\mathrm{f}-p_0), \tag{10}$$

where d_p is the diameter of piston, δ_1 is the oil film thickness between piston and cylinder block, μ is the kinetic viscosity of oil, l_1 is the overlap length of piston and cylinder block, p_0 is the pressure inside pump shell chamber, d_d is the diameter of leakage hole in piston, v_p is the velocity of piston, δ_2 is the oil film thickness between swash plate and slipper, r_1 is the radius of chamber in slipper, r_2 is the radius of the slipper, l_d is the length of leakage hole in piston, δ_3 is the oil film thickness between cylinder block and valve plate, R_1 and R_2 are the inside and outside radii of inside valve plate seal ring, respectively, R_3 and R_4 are the inside and outside radii of outside valve plate seal ring, respectively. The structure of the valve plate is shown Fig. 6.

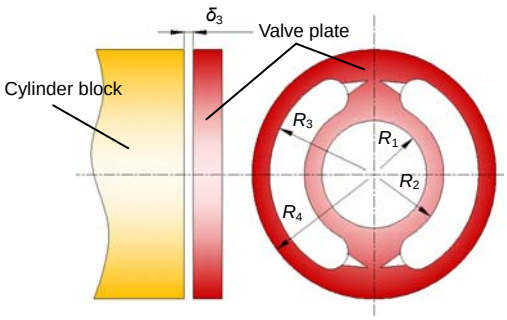

Fig. 6 Structure of the valve plate

The bulk modulus of oil is measured in the flow ripple test-rig using the cross correlation function method (Fig. 7). Experimental results of the fluid bulk modulus were used in the model to achieve a high accuracy result.

2.2 Multi-cylinder model of pumping dynamics

The flow ripple of a multi-cylinder pump is due to the discontinuity in discharge flow rate from the piston and its governing pumping mechanism. The flow rate at the pump discharge port is the sum of the discharge flow rates of each individual piston connecting to the discharge kidney port, which is

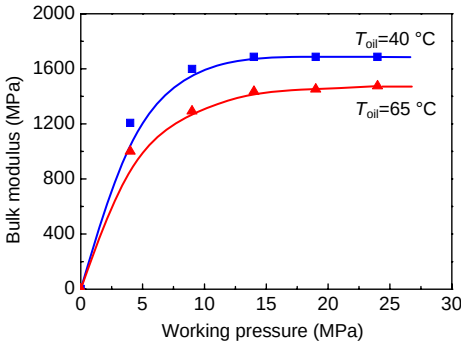

Fig.7 Bulk modulus of oil tested according to working pressure and temperature

written as $q_p = \sum_{i=1}^{9}(-q_{Hi})$, where q_{Hi} is the discharge flow rate of individual piston connecting to the discharge kidney port. So the multi-cylinder model of pumping dynamics combines several single cylinder models vectorially to produce the required effect. Each piston is separated from the previous one by a phase angle equal to a separation angle of 360/9 degrees for a nine-piston pump. In addition, as the volumetric loss through the gap between cylinder block and valve plate is the effect of the multi-piston, this flow rate is added after the connecting point of the flow rate from the piston chambers in the multi-cylinder pump model.

The pressure pulsations, which are the major source of system noise propagating through the fluid in the pipelines resulting in the vibration of pipes and any connected equipment, are affected not only by the flow ripple of the pump but also by the system parameters. So the system environment of the pump was built by adding the load of a throttle valve and the pipelines. The flow rate through the throttle valve is expressed by the classical orifice equation given by

$$q_v = C_v A_v \sqrt{\frac{2}{\rho}(p_H - p_T)}, \tag{11}$$

where q_v is the flow rate of the throttle valve, C_v is the discharge coefficient of the throttle valve, A_v is the discharge area of the throttle valve, p_H is the discharge pressure of pump, and p_T is the pressure of tank.

The flow in the pipeline is influenced by the fluid discontinuity and fluid bulk modulus, and is expressed as

$$q_p - q_v = \frac{V_t}{K_e}\frac{dp_H}{dt}, \tag{12}$$

where q_p is the flow rate of the pump, V_t is the volume of pipeline.

Therefore, the flow characteristics of the relationship between the multi-cylinder and the pump working system can be evaluated with

$$\frac{V_t}{K_e}\frac{dp_H}{dt} + C_v A_v \sqrt{\frac{2}{\rho}(p_H - p_T)} = \sum_{i=1}^{9}(-q_{Hi}). \tag{13}$$

The multi-cylinder model of pumping dynamics with a hydraulic system is shown in Fig. 8.

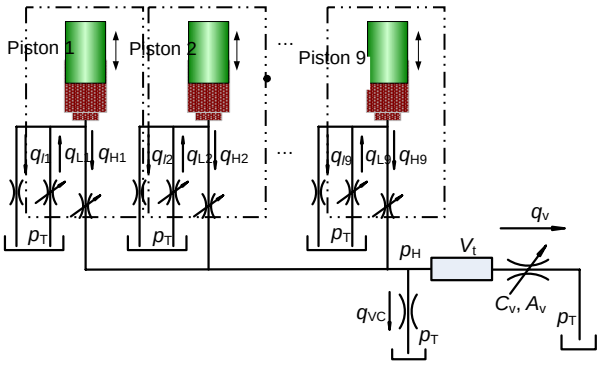

Fig. 8 Model of the whole pump with hydraulic system

The mathematical model of pumping dynamics consists of a set of differential and algebraic equations. These are to be solved using numerical techniques during simulation. MATLAB/SIMULINK(R) was chosen for simulation in this study considering its wide usage and availability. The multi-cylinder pump model was developed as a combination of various subsystem models. The S-functions corresponding to each subsystem calculate the required state space variables for a set of inputs and initial conditions.

3 Accuracy of mathematical model

3.1 Introduction of the test-rig

To study the accuracy of the pumping dynamics model, a test-rig of pump flow ripple was built, which can measure the flow ripple, pressure pulsation of the pump and the fluid bulk modulus of oil. The flow

ripple of a pump is a kind of high frequency signal, and it is hardly being tested directly. So the flow ripple has been calculated based on the pressure pulsation measured by the pressure sensor in the test-rig. The basic principle function for testing the source flow ripple at frequency domain is given by (Johnston, 1987)

$$P_X = Q_S \frac{Z_0 Z_S}{Z_0 + Z_S} \frac{\exp(-\gamma l) + \rho_T \exp[-\gamma(2l - x)]}{1 - \rho_S \rho_T \exp(-2\gamma l)}, \quad (14)$$

where P_X is the pressure at pressure sensor position X, Q_S is the source flow ripple, Z_0 is the characteristic impedance of the pipe, Z_S is the source impedance, γ is the transfer function, l is the length of pipeline, ρ_T is the termination reflection coefficient, ρ_S is the source reflection coefficient. Supposing the discharge passageway of the pump to be a uniform pipe, the source impedance of the pump is given as

$$Z_S = \frac{\rho c_0}{A_c}\left(1 + \frac{\omega_{vp}}{2j\omega}\right)^{\frac{1}{2}}, \quad (15)$$

where $\omega_{vp} = \frac{r_{op}^2}{8\nu}$, c_0 is the speed of pressure wave, A_c is the effective cross-sectional area, r_{op} is the effective cross-sectional radius, ν is the kinematical viscosity of oil.

The test-rig of the flow ripple test was built based on ISO 10767-1-1996 (1996). Pressure sensors were installed in the straight pipe at the outlet of the testing pump. An auxiliary pump was used as the secondary source for analyzing the source impedance of the testing pump. A throttle valve was used to adjust the working pressure levels. In addition, the working condition parameters, such as flow rate, temperature, rotation speed of pump, were also tested. Fig. 9 is the photo of the test-rig.

The flow ripple produced by the pump is influenced by the pumping mechanism and the fluid properties, and is independent of the dynamic characteristics of the circuit to which the pump is connected. Thus the flow ripple is more suitable as the measurement of the pump fluid noise level. Thus, the source flow ripple of the pump is evaluated by a mathematical model and compared with experimental results.

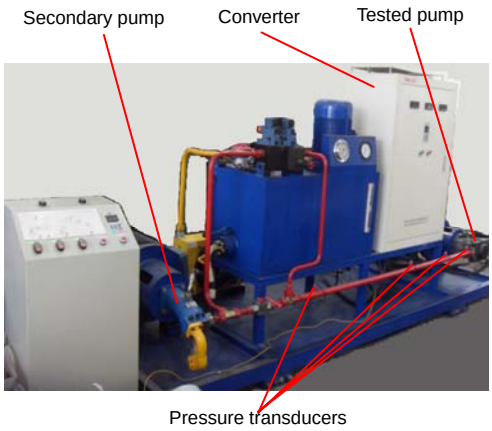

Fig. 9 The photo of the flow ripple test rig of pump

3.2 Precision of the mathematical model

With the test-rig above, the comparison of pressure pulsation and flow ripple between experimental results and simulation results has been done with the nine-pistons pump working at a pressure of 19.0 MPa and a rotation speed of 2000 r/min. As shown in Fig. 10, the thick curve (simulation result) agrees the thin curve (experimental result) very well, which means the improved mathematical model has high precision for predicting the output pressure of the axial piston pump.

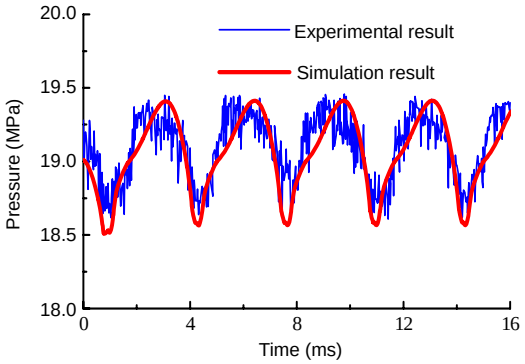

Fig. 10 Comparison of pressure pulsation between simulation result and experimental result

The flow ripple of the pump was calculated based on the pressure pulsation result. The comparison between simulation and experimental results is shown in Fig. 11, the maximum flow ripple amplitude of the experimental result is about 15 L/min, the mathematical model simulation result is about 14.6 L/min. Compared with the total pump flow rate of 80 L/min, the flow ripple rate of the experimental

result is about 19%, and the flow ripple rate of the mathematical result is about 18.3% (Table 1). Therefore, the error of the multi-cylinder pump model in the flow ripple prediction is only about 3%. So the accuracy of the mathematical model is acceptable.

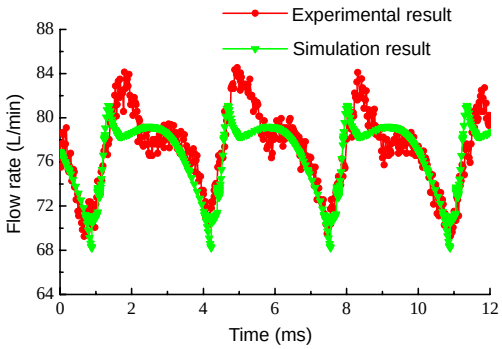

Fig. 11 Comparison of flow ripple between model simulation and experimental test

Table 1 Data comparison of experimental result and simulation result

Method	Amplitude of flow ripple (L/min)	Flow ripple rate (%)
Mathematical result	14.6	18.3
Experimental result	15.0	19.0

4 Optimization of the cross angle

There is a significant pressure differential between the intake port and the discharge port of the valve plate. Consequently, a reverse flow is established during the trapping period between ports. This together with the piston motion causes overshoot or undershoot in cylinder pressure, which is one of the main reasons for flow ripple. The cross angle of the valve plate has a close influence on the overshoot or undershoot and the flow ripple by changing the pressure differential between the intake port and the discharge port of the valve plate. The cross angle (φ_0), is the angle between the axis of valve plate symmetry and the line of the top dead point to bottom dead point of the cylinder block, which fixes the angular position of the valve plate (Fig. 12). The pre-compression angle of the valve plate is determined by the cross angle. The relationship of the cross angle and the pre-compression angle of the valve plate for the testing pump is shown in Table 2. The pump was simulated in the same working condition with a pressure of about 19.0 MPa and a rotation speed of 2000 r/min.

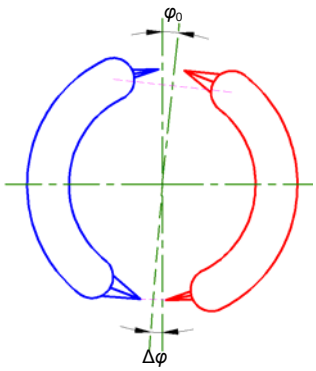

Fig. 12 The cross angle of valve plate

Table 2 The relationship of the cross angle and the pre-compression angle of valve plate

Cross angle	Pre-compression angle	Cross angle	Pre-compression angle
0°	−0.5°	6°	5.5°
2°	1.5°	8°	7.5°
4°	3.5°		

4.1 Influence of flow ripple

Fig. 13 shows the flow ripple at the pump outlet at different cross angles of the valve plate. The upper peak value of the flow ripple grows with an increasing cross angle. When the cross angle is 0°, there is almost no obvious upper peak. When the cross angle reaches 8°, the upper peak value of the flow ripple is quite clear at about 7.8 L/min. On the other hand, the lower peak valve of the flow ripple has the opposite changeover rules so that the peak valve decreases with an increase in the cross angle. The lower peak valve of the flow ripple is about 3.8 L/min at a cross angle of 0°. But when the cross angle grows to 8°, the lower peak of the flow ripple almost disappears.

In fact, both the upper and lower peaks of the flow ripple will result in the vibration of pipes or connected equipment. Therefore, there is a balance between the upper and lower peaks of the flow ripple so as to achieve the lowest damage. Fig. 14 gives the amplitude of the flow ripple and flow ripple rate changing with the cross angle, based on the previous results. When the cross angle is 2.2° with a pre-compression angle of 1.7°, the amplitude of the flow ripple and flow ripple rate reach a minimum

value. So the valve plate can be best designed at this cross angle to lower the flow ripple of the pump.

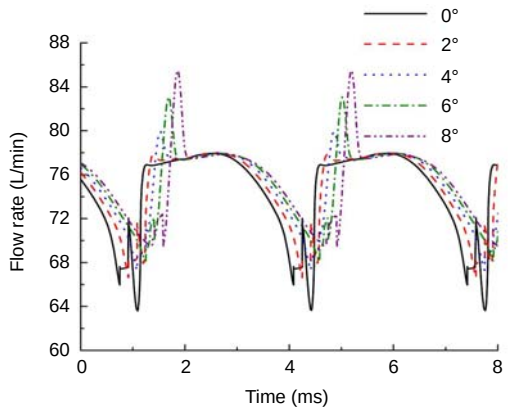

Fig. 13 The flow ripple of pump at different cross angles

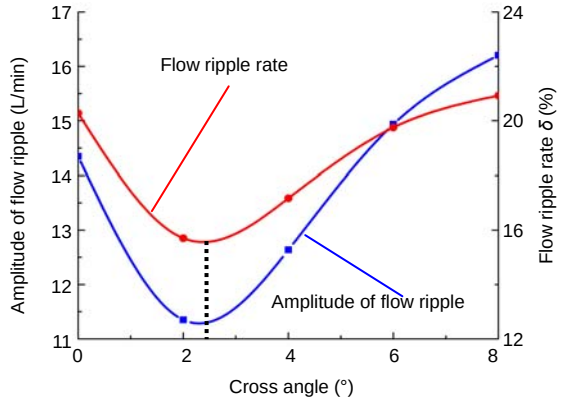

Fig. 14 The amplitude of flow ripple and flow ripple rate changing with the cross angle

4.2 Influence of overshoot or undershoot in cylinder pressure

Relatively low levels of delivery flow ripple are created when pump cylinders are optimally pre-compressed with an optimal cross angle. In this ideal situation, the pressure in each cylinder matched the delivery pressure on meeting the delivery port and so rapid cylinder flows to and from the delivery chamber are eliminated.

To achieve optimal or near-optimal pre-compression over a wide range of operating conditions, the cylinder pressure was simulated with different cross angles. Fig. 15 shows the plots of the pressure profile inside the piston chamber. The pressure inside the piston chamber is pre-compressed/expanded because of the cross angle of the valve plate and the fluid delivery delay. There are four pressure

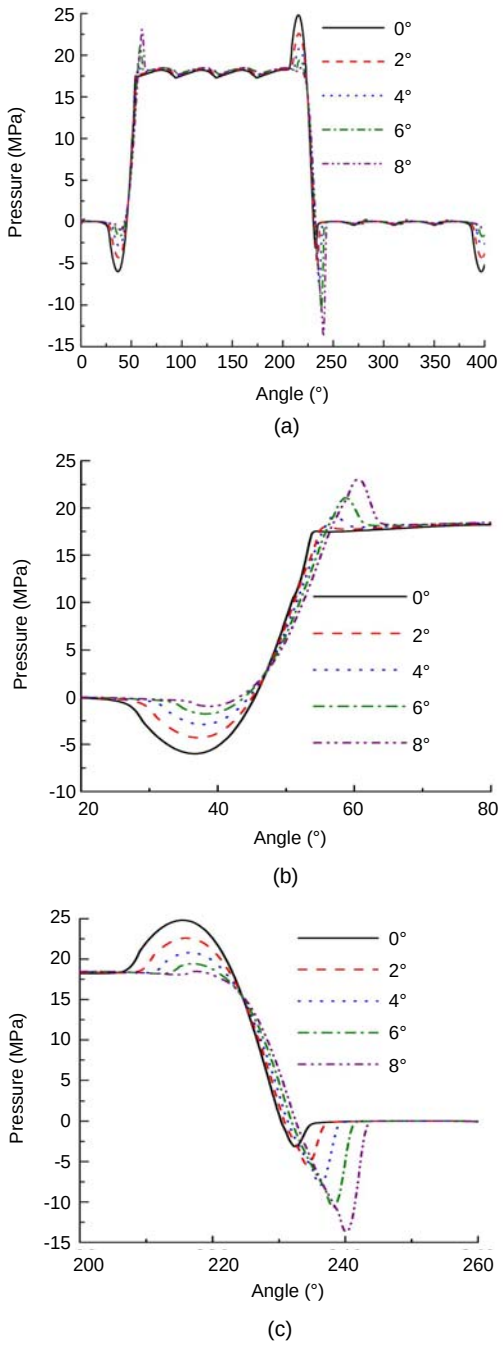

Fig. 15 (a) Pressure inside the piston chamber; (b) Pressure changing from the low to high pressure port; (c) Pressure changing from the high to low pressure

overshoots or undershoots in the piston chamber in one rotation cycle. The pressure overshoot or undershoot appears when the piston is rotating from the low to high pressure port or from the high to low pressure port. The overshoot and undershoot values change with the cross angle of the valve plate. Cavitations

might appear if the undershoot is significant and falls below the atmospheric pressure. On the other hand, the overshoot inside the piston chamber will lead to a transfer of fluid back to the suction port and a consequent reduction in the pump volumetric efficiency. Also, a force pulsation is likely added to the cylinder block to cause the tipping and overturning moment ripple on the cylinder block.

To achieve the optimal cross angle and the pre-compression angle of the valve, the four overshoots or undershoots value changing with the cross angle was analyzed (Fig. 16). When the cross angle is 2.7°, the total overshoot reaches the minimum value. So the corresponding optimal pre-compression angle is 2.2° to achieve the lowest overshoot or undershoot in cylinder pressure.

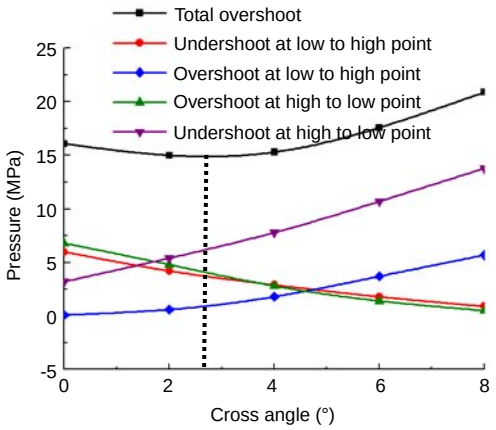

Fig. 16 The four overshoots or undershoots value changing with the cross angle

When considering both the flow ripple and the cylinder pressure of the pump, the cross angle is set to be 2.2° to 2.7° with a pre-compression angle of 1.7° to 2.2° and then the pumping dynamics characteristics can obtain the best result.

5 Conclusion

In this study of the pumping dynamics of an axial piston pump, the single cylinder model of pumping dynamics was improved. Particular attention has been paid to the design influences of key parts of the valve plate, such as relief groove, pre-compression/expansion and fluid inertia effect in the unsteady flow in the relief groove and cylinder on the pump delivery flow ripple. Some important parameters, such as the discharge area, discharge coefficient, fluid bulk modulus, were especially analyzed using numerical methods or by experiment-based estimation. In addition, a multi-cylinder model of pumping dynamics was built by establishing the system model of the pump.

The accuracy of the pumping dynamics model was analyzed using the test-rig of the flow ripple. The simulation results for pressure pulsation and flow ripple agree well with the experimental results. And the accuracy of the mathematical model is acceptable.

The pumping dynamics characteristics, including the flow ripple and the cylinder pressure of the pump, were analyzed based on the pumping dynamics model. The cross angle and the pre-compression angle of the valve plate were optimized. Considering both the flow ripple and the cylinder pressure of the pump, the cross angle is set to be 2.2° to 2.7° with a pre-compression angle of 1.7° to 2.2°, and then the pumping dynamics characteristics can achieve the best result.

In the future, experimental work with the cross angle of the valve plate will be made to further improve the simulation results. Also, the pressure in the piston chamber will be measured using a micro pressure sensor to compare with the simulation results.

References

Bebber, D., Murrenhoff, H., 2002. Improving the wear resistance of hydraulic machines using PVD-coating technology. *Ölhydraulik und Pneumatik*, **46**(11-12):1-35 (in German).

Becher, D., 2004. Untersuchungen an Einer Axialkolbenpumpemit Ringsystem Zur Mingerung von Pulsationen. PhD Thesis, TU Dresden (in German).

Bobzin, K., Lugscheidera, E., Maesa, M., Goldb, P.W., Loosb, J., Kuhnb, M., 2004. High-performance chromium aluminium nitride PVD-coatings on roller bearings. *Surface & Coatings Technology*, **188-189**:649-654. [doi:10.1016/j.surfcoat.2004.07.030]

Edge, K.A., Darling, J., 1988. A Theoretical Model of Axial Piston Pump Flow Ripple. Design Modelling and Control of Pumps/First Bath International Fluid Power Workshop, Bath, p.113-136.

Edge, K.A., Johnston, D.N., 1990a. 'Secondary source' method for the measurement of pump pressure ripple characteristics. Part 1. Description of method. *Proceedings of the Institution of Mechanical Engineers Part A. Journal of Power and Process Engineering*, **204**(11):33-40. [doi:10.1243/PIME_PROC_1990_204_006_02]

Edge, K.A., Johnston, D.N., 1990b. Secondary source method for the measurement of pump pressure ripple characteristics. Part 2: Experimental results. *Proceedings of the Institution of Mechanical Engineers Part A. Journal of Power and Energy*, **204**(11):41-46. [doi:10.1243/PIME_PROC_1990_204_007_02]

Ericson, L., Palmberg, J.O., 2007. The Source Admittance Method for Pumps with Complex Outlet Channels. The Tenth Scandinavian International Conference on Fluid Power, Tampere, p.279-293.

Guo, W., Wang, Z., 1996. Analysis for the real flowrate of a swashplate axial piston pump. *Journal of Beijing University of Aeronautics and Astronautics*, **22**(2):223-227.

Huang, C., Ivantysynova, M., 2003. A New Approach to Predict the Load Carrying Ability of the Gap between Valve Plate and Cylinder Block. Proceedings of Bath Workshop on Power Transmission and Motion Control, Bath, p.225-239.

ISO 10767-1, 1996. Hydraulic Fluid Power—Determination of Pressure Pulsation Levels Generated in Systems and Components—Part 1: Precision Method for Pumps.

Ivantysyn, J., Ivantysynova, M., 2001. Hydrostatic Pumps and Motors. Academia Books International, New Delhi, India, p.130-133.

Ivantysynova, M., Huang, C., 2002. Investigation of the Gap Flow in Displacement Machines Considering Elastohydrodynamic Effect. Fifth JHPS International Symposium on Fluid Power, Kyoto, p.219-229.

Ivantysynova, M., Huang, C., 2005. Thermal Analysis in Axial Piston Machines Using CASPAR. Proceedings of the Sixth International Conference on Fluid Power Transmission and Control, Hangzhou.

Johnston, D.N., 1987. Measurement and Prediction of the Fluid Borne Noise Characteristics of Hydraulic System. PhD Thesis, University of Bath.

Kazama, T., 2005. Numerical Simulation of a Slipper Model for Water Hydraulic Pumps/Motors in Mixed Lubrication. Proceeding of the 6th JFPS International Symposium on Fluid Power, Tsukuba.

Lasaar, R., Ivantysynova, M., 2001. Gap Geometry Variations in Displacement Machines and Their Effect on the Energy Dissipation. Proceedings of 5th International Conference on Fluid Power Transmission and Control, p.296-301.

Liselott, E., 2005. Measurement System for Hydrostatic Pump Flow Pulsations. MS Thesis, Linköping University, Sweden.

Lu, J., 2006. Pulsant Analysis of the Aero-plane Hydraulic Pump and Research on Reducing Vibration. MS Thesis, Beijing University of Aeronautics and Astronautics, China (in Chinese).

Manring, N.D., Zhang, Y.H., 2001. The improved volumetric efficiency of an axial-piston pump utilizing a trapped volume. *Journal of Dynamic Systems Measurement and Control, Transaction of the ASME*, **123**(3):479-487. [doi:10.1115/1.1389311]

Manring, N.D., Dong, Z., 2003. The impact of using a secondary swash-plate angle within an axial piston pump. *Journal of Dynamic Systems, Measurement and Control, Transaction of the ASME*, **126**(1):65-74. [doi:10.1115/1.1648313]

Meincke, O., Rahmfeld, R., 2008. Measurements, Analysis and Simulation of Cavitation in an Axial Piston Pump. The 6th International Fluid Power Conference, TU Dresden, **2**:485-499.

Na, C., Yin, W., 2002. Design of valve plate of axial piston pump with compressible working medium. *Journal of Lanzhou University of Technology*, **28**(4):65-67 (in Chinese).

Rokala, M., Koskinen, K.T., Calonius, O., Pietola, M., 2008. Tribological Conditions between Swashplate and Slipper Pad in Variable Displacement Water Hydraulic Axial Piston Unit. The 6th International Fluid Power Conference Workshop, TU Dresden, p.301-314.

Sanchen, G., 2003. Auslegung Von Axialkolbenpumpen in Schrägscheibenbauweise Mit Hilfe der Numerischen Simulation. PhD Thesis, Aachen University, Germany (in German).

Wustmann, W., Helduser, S., Wimmer, W., 2008. CFD-simulation of the Reversing Process in External Gear Pumps. The 6th International Fluid Power Conference, TU Dresden, **2**:455-468.